Numerical study on characteristic of two-dimensional metal/dielectric photonic crystals*

Yi-Xin Zong(宗易昕)†, Jian-Bai Xia(夏建白)‡, and Hai-Bin Wu(武海斌)

State Key Laboratory of Semiconductor Materials, Institute of Semiconductors, Chinese Academy of Sciences, Beijing 100083, *China*

(Received 5 September 2016; revised manuscript received 24 November 2016; published online 10 March 2017)

An improved plan-wave expansion method is adopted to theoretically study the photonic band diagrams of two-dimensional (2D) metal/dielectric photonic crystals. Based on the photonic band structures, the dependence of flat bands and photonic bandgaps on two parameters (dielectric constant and filling factor) are investigated for two types of 2D metal/dielectric (M/D) photonic crystals, hole and cylinder photonic crystals. The simulation results show that band structures are affected greatly by these two parameters. Flat bands and bandgaps can be easily obtained by tuning these parameters and the bandgap width may reach to the maximum at certain parameters. It is worth noting that the hole-type photonic crystals show more bandgaps than the corresponding cylinder ones, and the frequency ranges of bandgaps also depend strongly on these parameters. Besides, the photonic crystals containing metallic medium can obtain more modulation of photonic bands, band gaps, and large effective refractive index, etc. than the dielectric/dielectric ones. According to the numerical results, the needs of optical devices for flat bands and bandgaps can be met by selecting the suitable geometry and material parameters.

Keywords: photonic crystal, plane-wave expansion method, flat band, photonic bandgap

PACS: 42.70.Qs, 02.60.Cb, 78.66.Bz, 41.20.Jb **DOI:** 10.1088/1674-1056/26/4/044208

1. Introduction

Recently, photonic crystal (PC) has been studied theoretically and experimentally and has aroused great interest in the optical field and developed rapidly. The active research area has been extended to M/D PC which is expected to obtain more particular characteristics than the traditional dielectric/dielectric (D/D) PCs.[1–9] Yablonovitch and John first proposed the photonic band gap (PBG) structures for achieving a complete control of the spontaneous emission.[10,11] Photonic crystals are artificial periodic materials with spatial variation of dielectric constant on the order of an optical wavelength, which can control radiation field and light propagation characteristics. Owing to the periodic structure of PCs, photonic band gap is obtained and offering the opportunity to achieve a complete optical confinement, which may modify the basic properties of PCs systems.[12] Due to the superior property of PBG in PCs, there appears great interest in using the PBG structures to design new optoelectronic devices, such as low threshold lasers, frequency filters, integrated photonic circuits, optical switches, and waveguides for guiding and filtering electromagnetic (EM) waves.[13–19] For example, Akahane *et al.*[13] demonstrated the high-quality factor photonic nanocavity in a 2D PC, by using the cavity with both high-quality factor and small modal volume. Erdiven[15] investigated the design and performance of novel communication system using 2D PCs, and showed those PC arrangements that appropriate for many optical applications such as high performance photonic integrated circuits. Menura *et al.*[16] modeled a nonlinear optical switching in a standard PC fiber infiltrated with carbon disulfide. They analyzed the propagation of ultrafast optical pulses in PC fibers, and makes it a good candidate for optical switching. Another interesting feature of PCs is the flat band, which enables a small group velocity of light in all crystal directions.[20,21] There is an enhancement effect when the group velocity of the eigenmode in PCs is small, especially the flat band is peculiar for 2D PCs to obtain a generation and a fairly large enhancement of radiation field.[22] It has been proved that the small group velocity in all crystal directions leads to the enhancement of light amplification more efficiently than that at the band gap. So the flat band can also make sense in the case of low-threshold photonic crystal lasers.[23,24] The 2D PCs can serve as an ideal structure because of the strong vertical confinement within the 2D plane, and the fabrication of 2D PC with band gap is much easier than that of 3D PC, especially in the visible or infrared region.[25,26] Thus, it is necessary to find more 2D PCs with certain PBG or flat band.

The EM waves in PCs can be classified into transverse electric (TE) and transverse magnetic (TM) modes, for which the electric and magnetic field are parallel to the hole or pole direction in the 2D PC respectively.[27] Unlike the dielectric constant for dielectric medium in D/D PC, the dielectric func-

*Project supported by the National Basic Research Program of China (Grant No. 2011CB922200) and the National Natural Science Foundation of China (Grant No. 605210010).

†E-mail: yxzong@semi.ac.cn

‡Corresponding author. E-mail: jbxia@semi.ac.cn

© 2017 Chinese Physical Society and IOP Publishing Ltd

tion of metallic medium in M/D PCs is frequency dependent, are approximately defined by the Drude formula,[22,28] and used in this work. In this model the dielectric function is $\varepsilon(\omega)=\varepsilon_\infty-\omega_p^2/(\omega(\omega+i\Gamma))$, where ε_∞ is the high-frequency dielectric constant, Γ is the damping coefficient and ω_p is the plasmon frequency.[28,29] For the sake of simplicity, we consider the lossless case in which the imaginary part in the dielectric function is omitted. The frequency dependence of the metallic medium's dielectric function caused difficulties in the numerical calculation.

The plane-wave expansion (PWE) method is straightforward for the numerical simulation of band structures of dielectric PCs.[30–32] However, when it is applied to the M/D PCs, the eigenvalue equation is nonlinear and hard to solve. In our previous work, we have proposed an improved PWE method and applied it to the photonic band structure of 2D M/D PCs.[33,34] It is shown that our improved PWE method is suitable to the numerical simulation of one-dimensional (1D), 2D, and three-dimensional (3D) M/D PCs. To the best of our knowledge, most of the numerical and experimental investigations for photonic crystals are restricted to D/D PCs and a lot of 2D D/D PCs-based devices have been developed.[35–41] So it is necessary to explore the photonic band structures for the 2D M/D PCs.

We begin this work with a simple introduction of the improved PWE method on the photonic band diagram of the 2D M/D PCs. Then we numerically simulate the relation between the PBGs and flat bands with the dielectric constant and filling factor. At last we compare the PBG and $n_{\rm eff}$ of the 2D D/D and M/D PCs.

2. Theoretical model of the PWE method to the 2D M/D PCs[33,34]

We choose two types of rectangular 2D M/D PCs structures to study in this work. One is the hole-type PCs with cylindrical dielectric-rods embedded in the metal background and the other is the cylinder-type PCs with cylindrical metal-rods embedded in the dielectric background. ε_a is the dielectric constant for the dielectric medium and $\varepsilon_m(\omega)$ is the dielectric function of the Drude type for the metallic medium,

$$\varepsilon_m(\omega)=\varepsilon_\infty-\frac{\omega_p^2}{\omega^2}. \tag{1}$$

2.1. TE modes

The electric field is along the hole or cylinder direction, which can be expanded as

$$\boldsymbol{E}=\sum_{\boldsymbol{G}}C_{\boldsymbol{G}}e^{i(\boldsymbol{k}+\boldsymbol{G})\cdot\boldsymbol{\rho}}\boldsymbol{i}_y, \tag{2}$$

where,

$$\boldsymbol{k}+\boldsymbol{G}=(k_x+F)\boldsymbol{i}_x+(k+G)\boldsymbol{i}_z,$$

$\boldsymbol{\rho}$ is the spatial vector in the $x-z$ plane ($\boldsymbol{\rho}=x\boldsymbol{i}_x+z\boldsymbol{i}_z$), $\boldsymbol{k}$ is the wave vector in the first Brillouin zone ($\boldsymbol{k}=k_x\boldsymbol{i}_x+k\boldsymbol{i}_z$) and $\boldsymbol{G}$ is the reciprocal lattice vector ($\boldsymbol{G}=F\boldsymbol{i}_x+G\boldsymbol{i}_z$, $G=2\pi m/d$, $F=2\pi n/b$ with $m=0,\pm1,\pm2,\ldots$; $n=0,\pm1,\pm2,\ldots$). According to the Maxwell equations, the magnetic field is

$$\begin{aligned}\boldsymbol{H}&=\frac{1}{\mu_0}\frac{1}{i\omega}\nabla\times\boldsymbol{E}\\&=\frac{1}{\mu_0\omega}\sum_{\boldsymbol{G}}C_{\boldsymbol{G}}e^{i(\boldsymbol{k}+\boldsymbol{G})\cdot\boldsymbol{\rho}}(\boldsymbol{k}+\boldsymbol{G})\times\boldsymbol{i}_y.\end{aligned} \tag{3}$$

From Eqs. (2) and (3) we can obtain the secular equation

$$(\boldsymbol{k}+\boldsymbol{G})^2C_{\boldsymbol{G}}=\frac{\omega^2}{c^2}\sum_{\boldsymbol{G}'}\varepsilon(\boldsymbol{G}-\boldsymbol{G}')C_{\boldsymbol{G}'}, \tag{4}$$

where $\varepsilon(\boldsymbol{G})$ is the 2D Fourier component of $\varepsilon(\boldsymbol{\rho})$. For the hole and cylinder PCs we have

$$\begin{aligned}\varepsilon(\boldsymbol{G})&=\frac{1}{db}\int_{-d/2}^{d/2}\int_{-b/2}^{b/2}d\rho\varepsilon(\boldsymbol{\rho})e^{-i\boldsymbol{G}\cdot\boldsymbol{\rho}}\\&=\begin{cases}\varepsilon_1 f+\varepsilon_2(1-f), & G=0,\\(\varepsilon_1-\varepsilon_2)\dfrac{2\pi}{db}\displaystyle\int_0^R\rho d\rho J_0(\boldsymbol{G}\cdot\boldsymbol{\rho}), & G\neq0,\end{cases}\end{aligned} \tag{5}$$

with $\varepsilon_1=\varepsilon_a$ and $\varepsilon_2=\varepsilon_m(\omega)$ for the hole PCs and $\varepsilon_2=\varepsilon_a$ and $\varepsilon_1=\varepsilon_m(\omega)$ for the cylinder PCs. Where b and d are the edge length of the unit cell along the x and z directions, respectively, with the shape ratio $d/b=0.9$, $f=(\pi r^2/db)$ is the filling factor, r denotes the radius of the rod.

2.2. TM modes

To obtain the eigenvalue equation for the TM modes, we first expand the magnetic field as

$$\boldsymbol{H}(\boldsymbol{r})=\sum_{\boldsymbol{G}}C_{\boldsymbol{G}}e^{i(\boldsymbol{k}+\boldsymbol{G})\cdot\boldsymbol{\rho}}\boldsymbol{i}_y. \tag{6}$$

From the Maxwell equations, we have

$$\nabla\times\boldsymbol{H}=-i\omega\varepsilon_0\varepsilon(\boldsymbol{\rho})\boldsymbol{E}. \tag{7}$$

Take the curl on Eq. (6), we gain

$$\boldsymbol{E}=\sum_{\boldsymbol{G}}D_{\boldsymbol{G}}e^{i(\boldsymbol{k}+\boldsymbol{G})\cdot\boldsymbol{\rho}}(\boldsymbol{k}+\boldsymbol{G})\times i_y, \tag{8}$$

and its curl

$$\begin{aligned}\nabla\times\boldsymbol{E}&=-i\sum_{\boldsymbol{G}}D_{\boldsymbol{G}}e^{i[k_xx+(k+G)z]}\left[k_x^2+(k+G)^2\right]i_y\\&=i\omega\mu_0\sum_{\boldsymbol{G}}C_{\boldsymbol{G}}e^{i(\boldsymbol{k}+\boldsymbol{G})\cdot\boldsymbol{\rho}}(\boldsymbol{k}+\boldsymbol{G})^2i_y.\end{aligned} \tag{9}$$

The curl of $\nabla\times\boldsymbol{H}$ can also be obtained as

$$\nabla\times(\nabla\times\boldsymbol{H})=\sum_{\boldsymbol{G}}C_{\boldsymbol{G}}e^{i(\boldsymbol{k}+\boldsymbol{G})\cdot\boldsymbol{\rho}}(\boldsymbol{k}+\boldsymbol{G})^2i_y. \tag{10}$$

From Eqs. (7)–(10), we obtain

$$D_{\boldsymbol{G}}=-\frac{\omega\mu_0}{(\boldsymbol{k}+\boldsymbol{G})^2}C_{\boldsymbol{G}}, \tag{11}$$

and the secular equation

$$(\boldsymbol{k}+\boldsymbol{G})^2 C_{\boldsymbol{G}} = \left(\frac{\omega}{c}\right)^2 \sum_{\boldsymbol{G}'} B_{kg}\varepsilon(\boldsymbol{G}-\boldsymbol{G}')C_{\boldsymbol{G}'}, \quad (12)$$

where

$$B_{kg} = \frac{(\boldsymbol{k}+\boldsymbol{G})\cdot(\boldsymbol{k}+\boldsymbol{G}')}{(\boldsymbol{k}+\boldsymbol{G}')^2}. \quad (13)$$

The expression of $\varepsilon(\boldsymbol{G})$ is given in Eq. (5).

Unlike the traditional PWE method, this improved method enables us to obtain the secular equations of 2D M/D PCs without solving the nonlinear equation. The resulting secular equations can be solved by using the LAPACK package and the band structures of M/D PCs can be obtained.[42]

3. Photonic band structure of 2D M/D PCs

Based on the above theoretical model, in this section we will first investigate the photonic band structures of both polarization modes for 2D M/D PCs. And then we will analyze the dependence of flat bands and PBGs on the dielectric constant (ε_a) and filling factor (f).

3.1. The flat band of 2D M/D PCs

Firstly, we choose the hole-type PCs to study the characteristics of flat band in terms of two parameters mentioned above. Throughout this paper the normalized frequency $\Omega = \omega d/2\pi c$ and the normalized plasmon frequency $\Omega_p = \omega_p d/2\pi c$ are used.

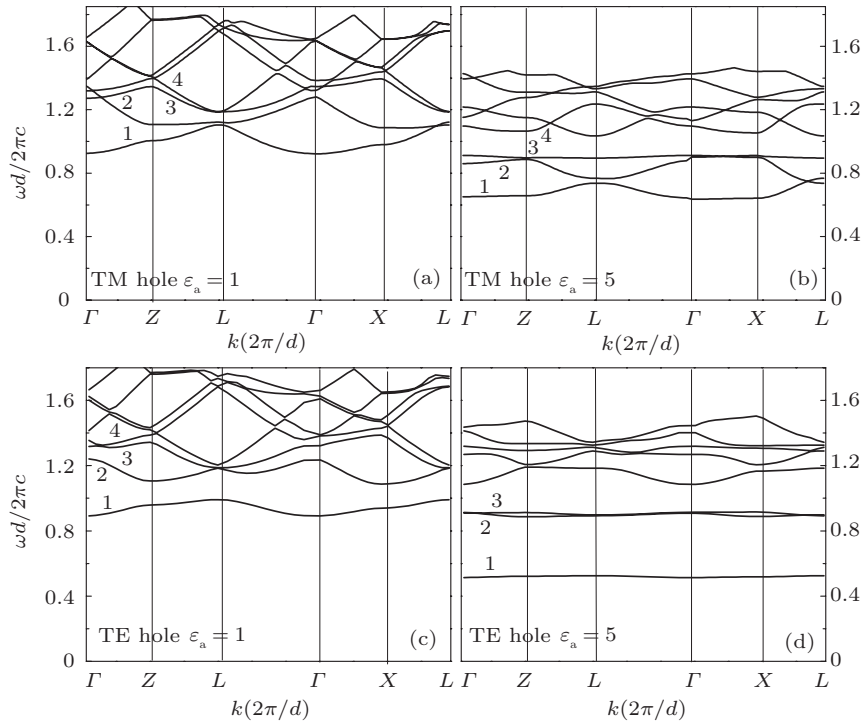


Fig. 1. The photonic band structure of the M/D hole PCs with $\Omega_p = 1$ and $f = 0.113$. (a) TM modes, $\varepsilon_a = 1.0$; (b) TM modes, $\varepsilon_a = 5.0$; (c) TE modes, $\varepsilon_a = 1.0$; (d) TE modes, $\varepsilon_a = 5.0$.

Figure 1 shows the band structures of the 2D M/D hole PCs with $\Omega_p = 1$, $f = 0.113$ and the two different dielectric constant ($\varepsilon_a = 1, 5$). The band structure is drawn in directions through four symmetry points: Γ, Z, L, and X. These four points represent the special (k_x, k_z) points $(0,0)$, $(0,0.5)$, $(0.5,0.5)$, and $(0.5,0)$ in the first Brillouin zone with the unit $2\pi/b$ and $2\pi/d$ in the x and z directions, respectively. We find that band-3 in Fig. 1(b) and band-1, 2, 3 in Fig. 1(d) are relatively flat in all directions. Therefore the flat bands for both TE and TM modes can be obtained by increasing the dielectric constant, which meets the needs of low-threshold photonic crystal lasers for small group velocity to gain more field enhancement.[23] For the TE modes shown in Fig. 1(d) the first PBG is in the range of 0.525–0.886, while for the TM modes in Fig. 1(b) it is in the range of 0.897–1.065, which is narrower than that of TE modes. We find from Fig. 1 that more PBGs arise and band-edge frequency decreases when the dielectric constant increases. The cut-off frequency, which is the minimum frequency of the lowest band, is relatively large corresponding to the width of PBGs, there is no EM wave propagating below this frequency. In this work the cut-off frequency is separated from other PBGs and will be presented in Subsection 3.2.

The band structures with two different filling factors are shown in Fig. 2 for the case of $\Omega_p = 1$. When the filling factor increases from 0.11 to 0.36, for TM modes, the band-2 becomes flat and the flat band-3 becomes steep, and the FBG between the band-3 and band-4 closes; for TE modes, the band-3 and band-4 become flat and a FBG between the band-3 and band-4 opens. Meanwhile, the cut-off frequencies together with other bands for both TM and TE modes decrease.

According to the photonic band structures shown in

Figs. 1 and 2, the interaction of the radiation field with the 2D M/D PCs depends strongly on the geometry and material parameters. The flat band and wide PBG can be easily achieved in 2D PCs containing metallic mediums. We also note that for the same set of parameters the PBG of the TE modes is wider than that of the TM modes. The numerical results provide a theoretical guidance for band structure engineering by tailoring certain parameters.

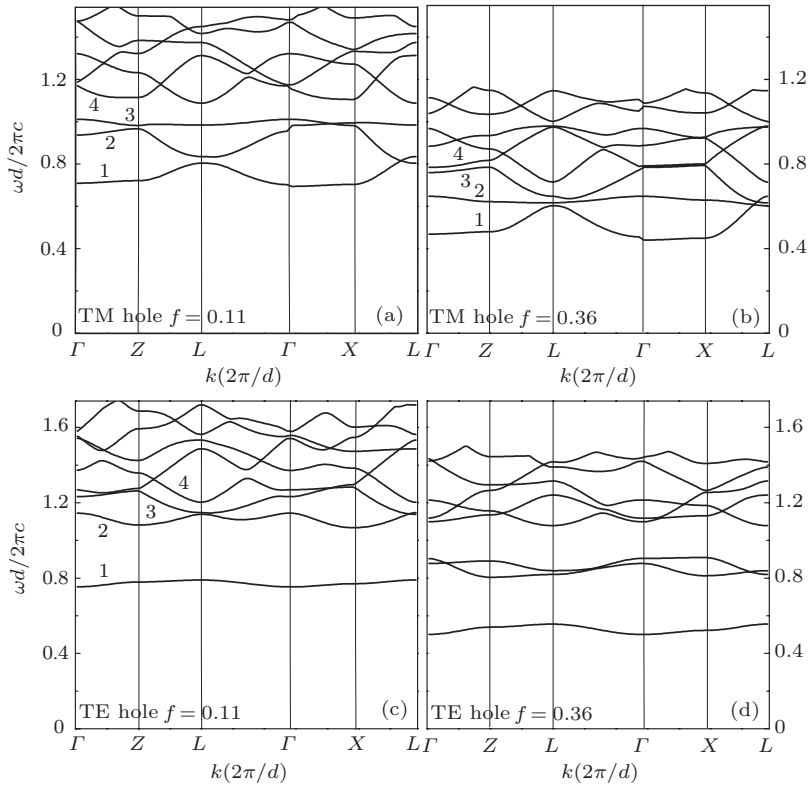


Fig. 2. The photonic band structure of the M/D hole PCs with $\Omega_p = 1$. (a) TM modes, $\varepsilon_a = 4.0$, $f = 0.11$; (b) TM modes, $\varepsilon_a = 4.0$, $f = 0.36$; (c) TE modes, $\varepsilon_a = 2.0$, $f = 0.11$; (d) TE modes, $\varepsilon_a = 2.0$, $f = 0.36$.

3.2. The PBG of 2D M/D PCs

In this subsection, we will discuss in detail the dependence of the cut-off frequency and the PBG on ε_a and f. We will mainly discuss the PBG among the lowest five modes in 2D hole and cylinder PCs.

3.2.1. Effect of dielectric constant on PBG

Firstly, we study the dependence of PBG on the dielectric constant of the dielectric medium in the hole- and cylinder-type PCs with the normalized plasmon frequency $\Omega_p = 1$, the filling factor $f = 0.113$. The ε_a is taken in a range of 1–20.

Figure 3 shows the PBG maps of the TM modes as ε_a is varied. For the hole-type PCs in Fig. 3(a), with the increase of ε_a, one PBG opens at $\varepsilon_a = 2.8$, i.e., the TM_{3-4} band gap. The width of TM_{3-4} band gap reaches to the maximum of $\Delta\Omega = 0.169$ at $\varepsilon_a = 10$, and then decreases slowly. That is to say, when ε_a increases, the EM wave will be scattered more strongly, and the PGBs are more likely to appear. The cut-off and gap-edge frequencies for the hole-type PC decreases monotonously when ε_a increases. However, for the cylinder-type PCs as shown in Fig. 3(b), there is no PBG present in this ε_a range and the cut-off frequency decreases with ε_a.

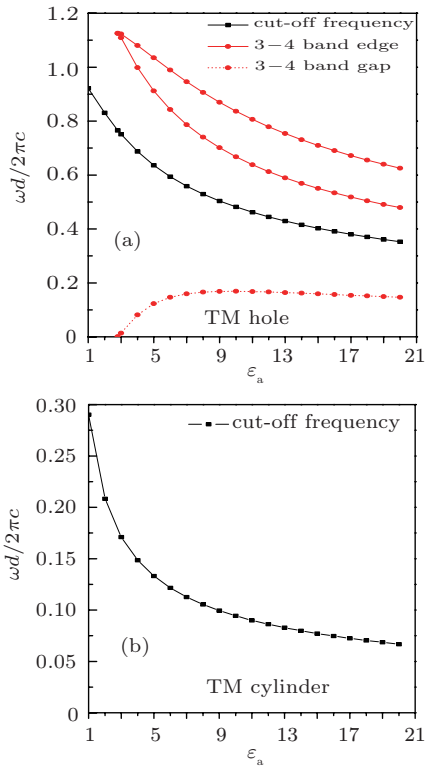


Fig. 3. (color online) The dependence of PBGs and band-edges on the dielectric constant for TM modes with $\Omega_p = 1$ and $f = 0.113$. (a) The hole-type PC; (b) The cylinder-type PC.

The PBG maps of the TE modes is shown in Fig. 4. There is a persistent open PBG for TE modes of the hole-type PCs, namely the TE_{1-2} band gap. The TE_{3-4} band gap does not open until $\varepsilon_a = 3.0$. With the increase of ε_a, both the widths of TE_{1-2} and TE_{3-4} band gaps increase to maximum and then decrease slowly. These two band gaps reach to their maximum width at $\varepsilon_a = 4$ and $\varepsilon_a = 9$, with a normalized width of 0.375 and 0.309 respectively. Comparing Fig. 4(a) with Fig. 3(a), we find the TE modes of the hole-type PCs show one more band gap than the TM modes. Besides, the overlap between the cut-off frequency and the lower 1–2 band-edge in Fig. 4(a) indicates that the first band is a flat band for the TE mode of the hole-type PC. The group velocity of flat bands is rather slow, which facilitates the laser action.[23] The case of the TE cylinder-type PCs is similar to that of the TM cylinder-type PCs in Fig. 3, there exists only the cut-off frequency, but no PBG.

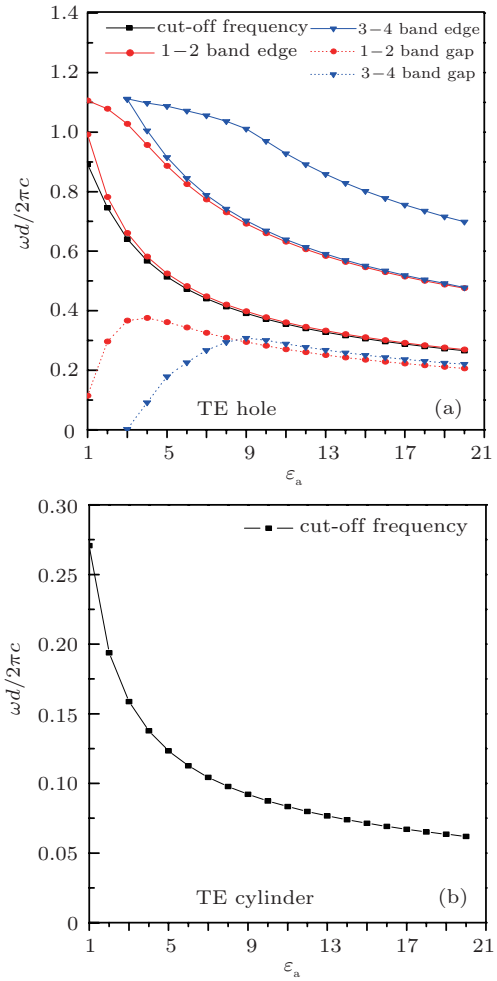


Fig. 4. (color online) The dependence of PBGs and band-edges on the dielectric constant for TE modes with $\Omega_p = 1$ and $f = 0.113$. (a) The hole-type PC; (b) The cylinder-type PC.

3.2.2. Effect of filling factor on PBG

In this subsubsection we investigate the PBG maps as a function of the filling factor $f = \pi r^2/db$. The variation scope of r/d is chosen within a range of 0.02–0.5, so that f varies from 0.001 to 0.706. The dependence of band PBGs and their gap-edges for the TM and TE modes on the filling factor are displayed in Figs. 5 and 6 respectively, with the normalized plasmon frequency $\Omega_p = 1$.

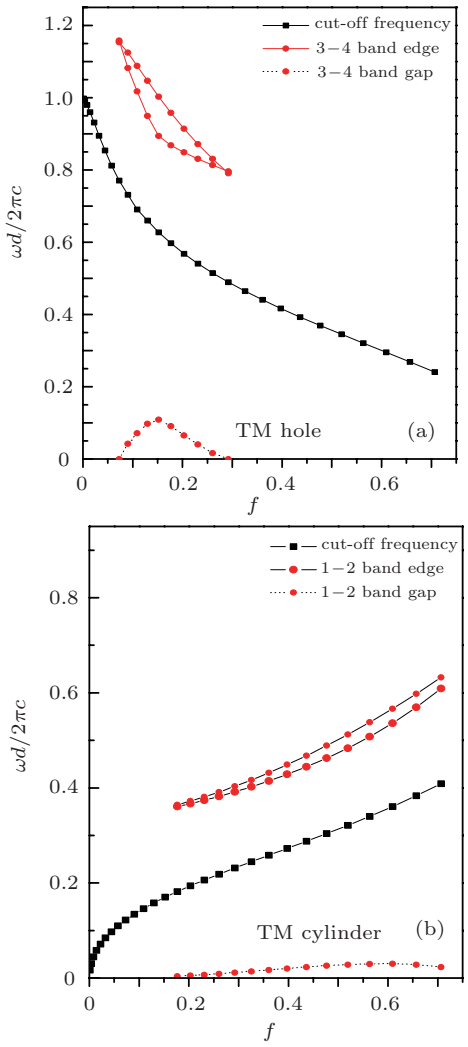


Fig. 5. (color online) The dependence of PBGs and band-edges on the filling factor for TM modes with $\Omega_p = 1$, $\varepsilon_a = 4$. (a) The hole-type PC; (b) The cylinder-type PC.

Figure 5 shows the PBG map of the TM modes with $\varepsilon_a = 4$. For the case of 2D M/D hole PCs in Fig. 5(a), we can find that the cut-off frequency is relatively large but decreases fast when f increases. The TM_{3-4} band gap opens at $f = 0.073$ and reaches to the maximum at $f = 0.15$. However, this PBG only exists when f is in the range of 0.073–0.29, and its maximum normalized width is 0.109, which is much smaller than the corresponding cut-off frequency. For the case of the cylinder-type PCs as shown in Fig. 5(b), a narrow TM_{1-2} band gap opens at $f = 0.177$ and reaches to the maximum of 0.03, which is much smaller than the cut-off frequency and varies smoothly with f. Contrary to the hole case, the cut-off frequency of the cylinder-type PCs increases with the filling factor f and the maximum width of the PBG is much smaller.

Comparing the PBG map of the TE modes in Fig. 6 with that of the TM modes in Fig. 5, we observed a similar trend of the cut-off frequency. In the case of the hole-type PCs, only one band gap shows up for the TM modes, and there are two band gaps for the TE modes, the TE_{1-2} and TE_{3-4} band gaps with the maximum normalized value of 0.390 and 0.267 respectively. As for the cylinder-type PCs, one band gap exists for the TM modes, and there is none for the TE modes.

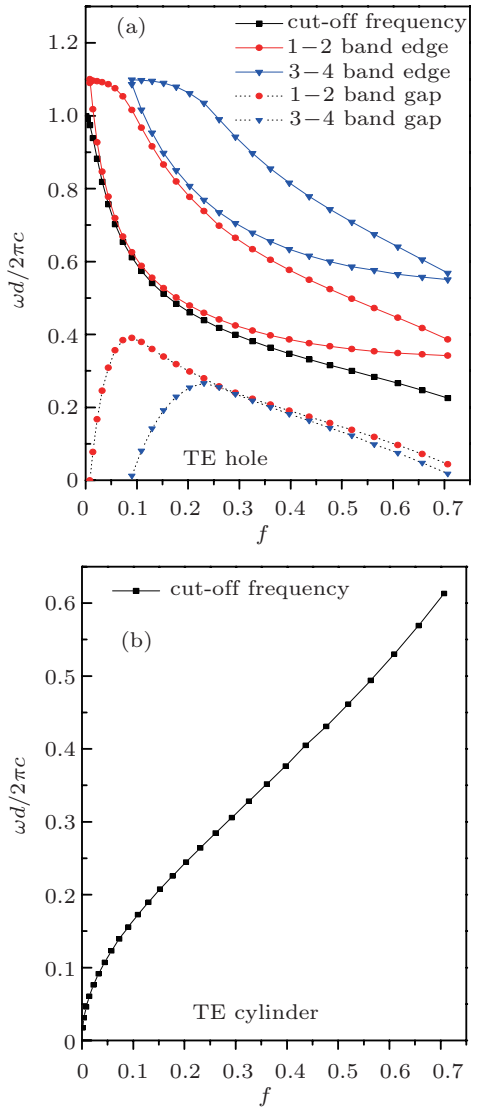


Fig. 6. (color online) The dependence of PBGs and band-edges on the filling factor for TE modes with $\Omega_p = 1$, $\varepsilon_a = 4$. (a) The hole-type PC; (b) The cylinder-type PC.

4. Comparison with the 2D D/D PCs

Owing to the frequency dependence on the dielectric function of metallic medium, unlike the D/D PCs, the M/D PCs exhibit particular properties. Sakoda calculated the photonic bands of the 2D D/D square air-rod lattice by the PWE method for the TE and TM modes.[43] and the transmission spectra (interference patterns) of the finite layers of the 2D square photonic lattice. He found that the effective refractive index estimated from the dispersion curves coincides with that from the interference patterns.

Since the wave vector of the incident plane-wave is parallel to the Γ–X direction, Sakoda concentrated on the band structure on the Γ–X direction. The calculated band gaps for the TE and TM modes are listed in Table 1 with the filling factor $f = 0.25$. With the same f and square dielectric-rod M/D lattice, we calculated the photonic bands in the Γ–X direction with $\varepsilon_a = 1, 5$, and obtained the band gaps also listed in Table 1.

Table 1. Comparisons of the band gaps of the D/D and M/D PCs for the TE and TM modes.

	D/D[43]	M/D ($\varepsilon_a = 1$)	M/D ($\varepsilon_a = 5$)
	Band gap	Band gap	Band gap
TE	0.353–0.387	0–0.399	0–0.185
	0.702–0.728	0.561–0.727	0.255–0.346
		1.027–1.081	0.468–0.500
		1.155–1.183	0.527–0.570
TM	0.354–0.401	0–0.439	0–0.208
	0.702–0.728	0.567–0.780	0.259–0.393
		1.080–1.102	0.501–0.534

Sakoda *et al.* also found that the group-velocity anomaly and decrease bring about the enhancement of light amplification[44] and a large reduction of lasing threshold.[45] They calculated the effective refractive index n_{eff} from the photonic bands

$$\frac{\mathrm{d}\omega}{\mathrm{d}k} = \frac{c}{n_{\text{eff}}}. \tag{14}$$

With the same parameters we also calculated the effective refractive index of the M/D PCs from the photonic bands, the effective band segments are used and the calculated results are listed in Table 2.

Table 2. Comparison of the n_{eff} of the D/D and M/D PCs for the TE and TM modes.

		D/D	M/D ($\varepsilon_a = 1$)	M/D ($\varepsilon_a = 5$)
	Band	n_{eff}	n_{eff}	n_{eff}
TE	1st	1.36	2.47	5.67
	2nd	1.43	1.41	3.50
	3rd	7.13	6.58	24.4
TM	1st	1.35	3.10	7.70
	2nd	1.38	1.47	3.80
	3rd	5.60	4.57	15.0

From Tables 1 and 2 we see that the M/D 2D PCs have more modulations, e.g., PBG, flat band, large band gap, small group velocity, and large effective refractive index, etc., than the D/D PCs, which are all beneficial to the photonic devices.

5. Conclusion

In this article we use our improved PWE method to simulate the flat band and the PBG properties of the 2D M/D PCs.

Based on the simulation results, we found that for the 2D PCs with metallic mediums, the cut-off frequency, flat band, and PBG can be tailored easily by adjusting the dielectric constant and filling factor. It is found that all the cut-off frequencies for both polarization modes are relatively large and always exist regardless of the material or geometry parameters. It is worth noting that the hole-type PCs show more PBGs than the corresponding cylinder-type ones, and the width of PBGs depend strongly on these two parameters. Meanwhile, from the simulation results, we found that contrary to the cylinder-type PCs cases, the PBGs for the hole-type PCs always exhibit a maximum width when the dielectric constant or the filling factor varies. At last, we compared the PBG and n_{eff} of the 2D D/D and M/D PCs. The M/D PCs have more modulations of photonic bands, flat band, large band gap, and large effective refractive index, etc., than the D/D PCs, which are all beneficial to the photonic devices. In conclusion, if suitable parameters, such as the dielectric constant and filling factor, are selected, desirable flat band and PBG structure can be realized or optimized to meet the needs of many optical devices made of the 2D M/D PCs.

References

[1] Joannopoulos J D, Villeneuve P R and Fan S 1997 *Nature* **386** 143
[2] Liang Q, Li D and Han 2012 *Materials* **5** 851
[3] Ignatov A I, Merzlikin A M, Levy M and Vinogradov A P 2012 *Materials* **5** 1055
[4] Thapa K B, Kumar R and Gupta A K 2010 *J. Optoelectron. Adv. Mater.* **12** 1670
[5] Qi L M, Yang Z Q, Lan F, Gao X and Li D Z 2010 *Chin. Phys. B* **19** 034210
[6] Naimi E K and Vekilov Y K 2015 *Solid State Commun.* **209** 15
[7] Song L, Zhong S and Liu S 2009 *Plasma Sci. Technol.* **11** 14
[8] Sakai O, Sakaguchi T and Tachibana K 2005 *Appl. Phys. Lett.* **87** 241505
[9] Fan C Z, Wang J Q, He J N, Ding P and Liang E J 2010 *Phys. Rev. Lett.* **104** 087401
[10] Yablonovitch E 1987 *Phys. Rev. Lett.* **58** 2059
[11] John S 1987 *Phys. Rev. Lett.* **58** 2486
[12] Wang L H and Yang S H 2013 *IEEE 2nd ISNE* 25
[13] Akahane Y, Asano T, Song B S and Noda S 2003 *Nature* **425** 944
[14] Arpin K A, Mihi A, Johnson H T, Baca A J, Rogers J A, Lewis J A and Braun P V 2010 *Adv. Mater.* **22** 1084
[15] Erdiven U 2015 *Optik* **126** 2044
[16] Munera N and Herrera R A 2016 *Opt. Commun.* **368** 185
[17] Wang D, Wu J Z and Zhang J X W 2016 *Chin. Phys. B* **25** 064202
[18] Shang G L, Fei G T and Li D Z 2015 *J. Phys. D: Appl. Phys.* **48** 435304
[19] Ye H, Zhang J Q N, Yu Z Y, Wang D L and Chen Z H 2015 *Chin. Phys. B* **24** 094214
[20] Lourtioz J M, Benisty H, Gerard J M, Maystre D and Tchelnokov A 2008 *Photonic Crystals: Towards Nanoscale Photonic Devices* (Berlin: Springer Press) pp. 198–224
[21] Gao B, Shi Z and Boyd R W 2015 *Opt. Express* **23** 6491
[22] Sakoda K 2005 *Optical properties of photonic crystals*, 2nd edn. (Berlin: Springer Press) pp. 151–154
[23] Inoue K, Kawai N and Sugimoto Y 2002 *Phys. Rev. B* **65** 121308
[24] Altug H and Vuckovic J 2005 *Appl. Phys. Lett.* **86** 111102
[25] Krauss T F, De La Rue R and Band S 1996 *Nature* **383** 699
[26] Notomi M, Yamada K, Shinya A, Takahashi J, Takahashi C and Yokohama I 2001 *Phys. Rev. Lett.* **87** 253902
[27] Zhang T, Shao W W, Li K, Liu X and Xu J 2007 *Opt. Commun.* **281** 1286
[28] Maier S A 2007 *Plasmonics: Fundamentals and Applications* (London: Springer Press) pp. 14–19
[29] Toader O and John S 2004 *Phys. Rev. E* **70** 046605
[30] Johnson S G and Joannopoulos J D 2001 *Opt. Express* **8** 173
[31] Shi S, Chen C and Prather D W 2004 *J. Opt. Soc. Am. A* **21** 1769
[32] Shen L F, He L and Wu L 2002 *Acta Phys. Sin.* **51** 1133 (in Chinese)
[33] Zong Y X and Xia J B 2015 *Sci. China-Phys. Mech. Astron.* **58** 077201
[34] Zong Y X and Xia J B 2015 *J. Phys. D: Appl. Phys.* **48** 355103
[35] Orlov A A, Zhukovsky S V and Iorsh I V 2014 *Photon. Nanostruct.* **12** 213
[36] Scalora M, Bloemer M J, Manka A S, Pethel S D, Dowling J P and Bowden C M 1998 *J. Appl. Phys.* **83** 2377
[37] Cheng C and Xu C 2009 *J. Appl. Phys.* **106** 033101
[38] Xiao S, Shen L and He S 2003 *Phys. Lett. A* **313** 132
[39] Sakoda K, Kawai N, Ito T, Chutinan A, Noda S, Mitsuyu T and Hirao K 2001 *Phys. Rev. B* **64** 045116
[40] Raman A and Fan S 2010 *Phys. Rev. Lett.* **104** 087401
[41] Chen J, Tang J, Han P and Chen J 2009 *J. Semicond.* **30** 043001
[42] Anderson E, Bai Z, Bischof C, Blackford S, Demmel J, Dongarra J, Du Croz J, Greenbaum A, Hammarling S and McKenney A 1999 *LAPACK Users' Guide*, 2nd edn. (Philadelphia SIAM Press) pp. 14–53
[43] Sakoda K 1997 *J. Opt. Soc. Am. B* **8** 1961
[44] Sakoda K 1999 *Opt. Express* **4** 167
[45] Sakoda K, Ohtaka K and Ueta T 1999 *Opt. Express* **4** 481